

REVIEW

Open Access



Defect Inspection Techniques in SiC

Po-Chih Chen^{1†}, Wen-Chien Miao^{2,4†}, Tanveer Ahmed¹, Yi-Yu Pan¹, Chun-Liang Lin⁴, Shih-Chen Chen^{2*}, Hao-Chung Kuo^{2,3*}, Bing-Yue Tsui¹ and Der-Hsien Lien^{1*}

Abstract

With the increasing demand of silicon carbide (SiC) power devices that outperform the silicon-based devices, high cost and low yield of SiC manufacturing process are the most urgent issues yet to be solved. It has been shown that the performance of SiC devices is largely influenced by the presence of so-called killer defects, formed during the process of crystal growth. In parallel to the improvement of the growth techniques for reducing defect density, a post-growth inspection technique capable of identifying and locating defects has become a crucial necessity of the manufacturing process. In this review article, we provide an outlook on SiC defect inspection technologies and the impact of defects on SiC devices. This review also discusses the potential solutions to improve the existing inspection technologies and approaches to reduce the defect density, which are beneficial to mass production of high-quality SiC devices.

Keywords: SiC, Killer defect, Defect inspection technology

Introduction

Owing to the rapid growth of power electronics market, SiC, a wide-bandgap semiconductor, emerges as a promising candidate to develop the next-generation power devices used in electric vehicles [1], aerospace [2] and power conversion applications [3, 4]. SiC-based power electronics offers several advantages over conventional devices made from Si or GaAs. Table 1 shows the physical properties of SiC compared with those of Si and GaAs as well as other wide-bandgap materials, such as GaN and diamond. Attributed to a wide bandgap (~ 3.26 eV for 4H-SiC), SiC-based devices can operate at higher electric fields and higher temperatures with a better reliability over Si-based power electronics. SiC also exhibits excellent thermal conductivity (about three times that of Si), which enables higher power density package for SiC

devices with better heat dissipation. Its superior saturation electron velocity (about two times that of Si) allows for higher frequencies of operation with lower switching losses than Si-based power devices [4, 5]. The outstanding physical properties of SiC make it very promising for the development of a wide range of electronic devices, such as power MOSFETs with high blocking voltage and low on-resistance [6–8] as well as Schottky barrier diodes (SBD) that can withstand large breakdown fields with small reverse leakage currents [9].

Improving SiC wafer quality is important for manufacturers as it directly defines the performance of SiC devices and thus, dictates the production cost. However, the growth of SiC wafers with low defect density remains very challenging. Recently, the evolution of SiC wafer fabrication has accomplished a difficult transition from 100 mm (4-inch) to 150 mm (6-inch) wafer. SiC needs to be grown in a high-temperature environment along with its high rigidity and chemical stability, which leads to a high density of crystallographic and surface defects in the grown SiC wafer, resulting in poor quality of substrates and subsequently fabricated epitaxial layers. Figure 1 summarizes various kind of defects in SiC and the process steps which these defects originate

*Correspondence: gary.sc.chen@foxconn.com; hckuo@faculty.nctu.edu.tw; dhlien@nycu.edu.tw

[†]Po-Chih Chen and Wen-Chien Miao have contributed equally to this work.

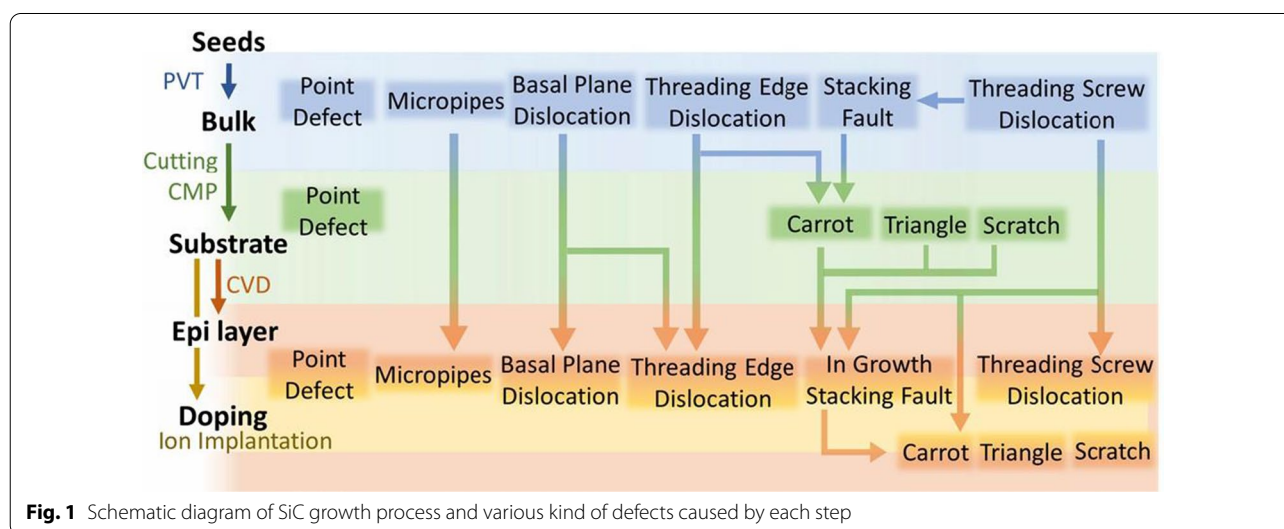
¹ Institute of Electronics, College of Electrical and Computer Engineering, National Yang Ming Chiao Tung University, Hsinchu 30010, Taiwan

² Semiconductor Research Center, Hon Hai Research Institute, Taipei 11492, Taiwan

Full list of author information is available at the end of the article

Table 1 Physical properties (room temperature values) of wide-bandgap semiconductors for power electronic applications in comparison with conventional semiconducting materials [10–12]

Property	Silicon	3C-SiC	4H-SiC	GaAs	GaN	Diamond
Bandgap energy (eV)	1.1	2.2	3.26	1.43	3.45	5.45
Breakdown field (10^6 Vcm^{-1})	0.3	1.3	3.2	0.4	3.0	5.7
Thermal conductivity ($\text{Wcm}^{-1} \text{ K}^{-1}$)	1.5	4.9	4.9	0.46	1.3	22
Saturated electron velocity (10^7 cm s^{-1})	1.0	2.2	2.0	1.0	2.2	2.7
Electron mobility ($\text{cm}^2\text{V}^{-1} \text{ s}^{-1}$)	1500	1000	1140	8500	1250	2200
Melting point ($^{\circ}\text{C}$)	1420	2830	2830	1240	2500	4000



from, and further discussion will be covered in the following section.

Various types of defects cause different degrees of deterioration to device performance and may even lead to complete failure of the device. In order to improve the yield as well as the performance, the technology of inspecting defects prior to device fabrication becomes very important. Therefore, a rapid, highly accurate, and non-destructive inspection technology plays an important role in the production line of SiC. In this article, we illustrate each type of defect and their impact on device performance. We also put forward a thorough discussion about the pros and cons of different inspection technologies. The analysis presented in this review article not only provides an overview of various defect inspection techniques available for SiC but also helps researchers to make a wise choosing among these techniques in the context of industrial applications (Fig. 2). Table 2 lists the acronyms of the inspection techniques and defects in Fig. 2.

Defects in SiC

Defects in SiC wafer are typically classified into two major categories: (1) crystallographic defects within the wafer and (2) surface defects at or near the wafer surface. As we further discuss in this section, crystallographic defects include Basal plane dislocations (BPDs), stacking faults (SFs), threading edge dislocations (TEDs), threading screw dislocations (TSDs), micropipes and grain boundaries, etc., as depicted in the cross-sectional schematic shown in Fig. 3a. Epitaxial layer growth parameters of SiC are very critical to the quality of wafer. Crystallographic defects and contaminations during growth processes [13] may extend into epitaxial layer and wafer surface to form various surface defects, including carrot defects, polytype inclusions, scratches, etc., or even convert to produce other defects [14], leading to detrimental effects on the final SiC devices.

The SiC epitaxial layers grown on 4° off-cut 4H-SiC substrate are the most common wafer type used today for a variety of device application. It is known that most

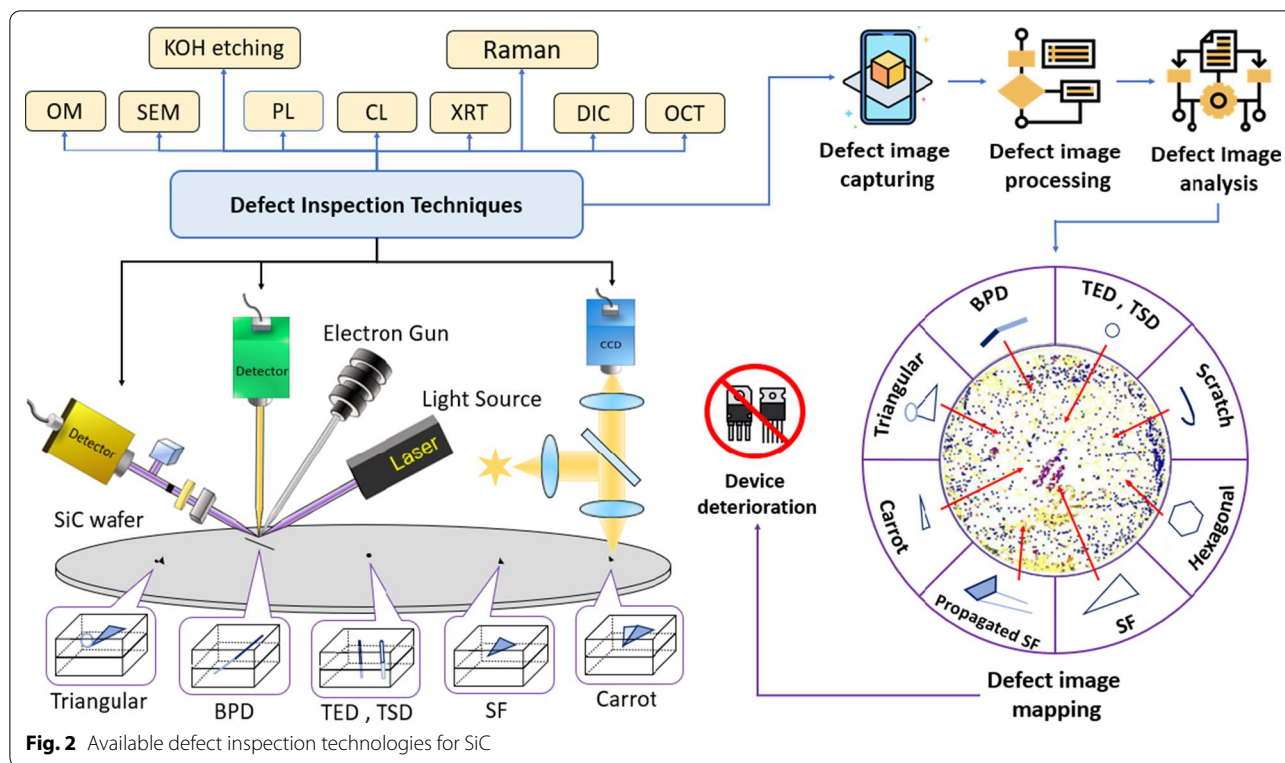


Fig. 2 Available defect inspection technologies for SiC

Table 2 The acronyms of the inspection techniques and defects in Fig. 2

SEM: Scanning electron microscopy	OM: Optical microscopy	BPD: Basal plane dislocation
DIC: Differential interference contrast	PL: Photoluminescence	TED: Threading edge dislocation
OCT: Optical coherence tomography	CL: Cathodoluminescence	TSD: Threading screw dislocation
XRT: X-ray topography	Raman: Raman spectroscopy	SF: Stacking faults

of the defects are oriented parallel to the growth direction, therefore, epitaxial growth of SiC at an off-cut angle of 4° on SiC substrates not only preserves the underlying 4H-SiC crystal, but also allows the defects to have a predictable orientation. In addition, total number of wafers, that can be sliced from a single boule, increases. However, lower off-cut angle may generate other type of defects, such as 3C-inclusions and in-grown SFs [18–21]. In the coming subsections, we discuss the details about each type of defects.

Crystallographic Defects

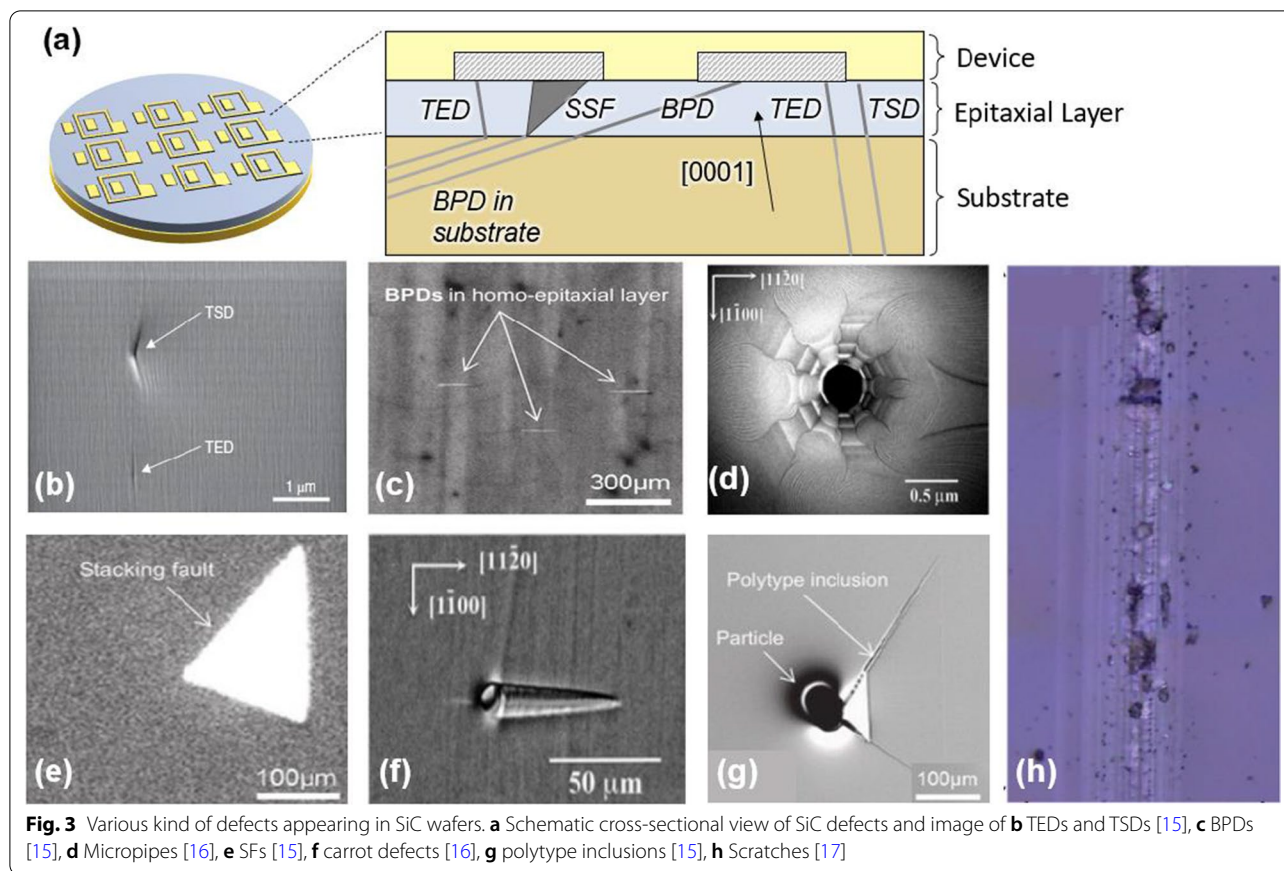
Threading Edge Dislocations (TEDs) and Threading Screw Dislocations (TSDs)

Dislocations in SiC are the main source for deterioration and failure of electronic devices [22–24]. Threading screw dislocations (TSDs) and threading edge dislocations (TEDs) both run along the [0001] growth axis with different Burgers vectors of <0001> and 1/3<11–20>, respectively.

Both TSDs and TEDs may extend from the substrate to the wafer surface and bring about small pit-like surface features [15], as shown in Fig. 3b [25]. Typically, density of TEDs is about 8000–10,000 1/cm², which is almost 10 times larger than that of TSDs. An extended TSD, where the TSD extends from the substrate to the epitaxial layer, may transform into other defects on the Basal plane and propagate along the growth axis during the SiC epitaxial growth. Harada et al. show that TSDs are converted to the stacking faults (SFs) or carrot defects on Basal planes during the SiC epitaxial growth [26], while TEDs in the epilayer are shown to be converted from BPDs inherited from the substrate during epitaxial growth.

Basal Plane Dislocations (BPDs)

Another type of dislocations is Basal plane dislocations (BPDs), which lie in the [0001]-plane of the SiC crystal with Burgers vector of 1/3<11–20>. BPDs rarely appear



on the surface of SiC wafer [15]. These generally concentrate at the substrate with a density of 1500 1/cm^2 while their density in the epitaxial layer is only about 10 1/cm^2 . Kamei et al. have reported that the density of BPDs decreases with increasing SiC substrate thickness [26]. BPDs show line-shaped features when using photoluminescence (PL) inspection, as shown in Fig. 3c [15]. An extended BPD may transform into SFs or TEDs during the SiC epitaxial growth.

Micropipes

The common dislocations observed in SiC are the so-called micropipes, which are hollow threading dislocations propagating along the [0001] growth axis with a large $\langle 0001 \rangle$ component of the Burgers vector. The diameter of micropipes ranges from a fraction of a micron to tens of microns. Micropipes show large pit-like surface features on the surface of SiC wafer [15]. Spirals which emanate from the micropipes, appearing as screw dislocations, are shown in Fig. 3d [16, 27]. Typically, the density of micropipes is around $0.1\text{--}1 \text{ 1/cm}^2$ and it continues to decrease in commercial wafers.

Stacking Faults (SFs)

Stacking faults (SFs) are defects with disarray of stacking sequence in SiC Basal planes. SFs may appear inside epitaxial layer by inheriting SFs in the substrate [15, 28, 29], or be associated with the transformation of extended BPDs and extended TSDs. Typically, the density of SFs is lower than 1 per cm^2 and these show triangle-shaped features by using PL inspection, as shown in Fig. 3e [15]. However, various types of SFs can be formed in SiC, such as Shockley-type SFs and Frank-type SFs, etc., since just a small amount of stacking energy disorder between crystal plane may lead to considerable irregularities in the stacking sequence [30].

Point Defects

The point defect is formed by vacancy or interstitial of a single lattice site or a few lattice sites, which have no spatial expansion. Point defects can occur in every production process, especially in ion implantation. However, they are difficult to be detected and the interrelationship between point defects and the transformation of other defects is too complicated, which beyond the scope of this review.

Other Crystallographic Defects

There exist a few more type of defects in addition to those described in the above subsections. The grain boundary is a distinct boundary caused by the lattice mismatch between two different SiC crystal types when they intersect [31]. The hexagonal void is a crystal defect in which there is a hexagonal cavity within a SiC wafer and it has been proven to be one of the sources of micropipe defects that make high voltage SiC devices fail [32]. Particle inclusions are caused by downfall particles during growth process, and their density can be greatly reduced by proper cleaning, careful operation of pumping and control of gas flow procedures.

Surface Defects

Carrots

Generally, surface defects are formed from extended crystallographic defects and contaminations. Carrot defect is a stacking fault complex with its length indicates the location of the TSD and SFs on Basal planes at both ends. The Basal faults are terminated by Frank partial dislocations, and the size of the carrot defect is related to the prismatic stacking faults [33]. The combination of these features forms the surface topography of a carrot defect, which resembles the shape of a carrot in its appearance with a density less than 1 per cm^2 , as shown in Fig. 3f [16]. Carrot defects are easily formed at polishing scratches, TSDs or an imperfection in the substrate [7].

Polytype Inclusions

Polytype inclusion, often referred to as triangular defect, is a lamellar inclusion of 3C-SiC polytype that extends to the surface of the SiC epilayer in a direction along Basal plane, as shown in Fig. 3g [15]. It may be generated by the downfall particles on the surface of the SiC epilayer during the epitaxial growth. As a result, the particle embedded in the epilayer and interferes with the growth process, creating a 3C-SiC polytype inclusion that shows acute-angled triangular surface feature with the particle located at the apex of the triangular region [15]. Many studies have also attributed the origin of polytype inclusions to surface scratches, micropipes and improper parameters of the growth process [34–36].

Scratches

Scratches are mechanical damages on the surface of SiC wafer formed during production processes, as shown in Fig. 3h [17]. Scratches on a bare SiC substrate may interfere with the growth of the epitaxial layer to create a high-density row of dislocations within the epitaxial layer, which are referred to as scratch traces [15], or scratches may become the basis for the formation of carrot defects

[37]. Therefore, proper polishing of SiC wafers is critical, as scratches can have a significant impact on the device performance when these are present in the active region of the device.

Other Surface Defects

Step bunchings are surface defects formed during the SiC epitaxial growth and bring about obtuse-angled triangular or trapezoidal features on the surface of the SiC epilayer. There are many other surface defects such as surface pits, bumps and stain. These defects are usually created by non-optimized growth processes and incomplete removal of polishing damage, resulting in significantly detrimental impact on the performance of devices.

Inspection Techniques

Quantifying the SiC substrate quality is an essential step before epitaxial layer deposition and device fabrication. After the epitaxial layer is formed, wafer inspection should be performed again to ensure that the location of defects is known, and their number is under control. Inspection techniques could be classified into surface inspection and subsurface inspection, depending on their ability to effectively extract structural information over or beneath the surface of the sample. As we further discuss in this section, in order to accurately identify the type of surface defects, KOH (potassium hydroxide) is usually used to visualize surface defects by etching them to a visible size under the optical microscope [38]. However, this is a destructive approach that cannot be used in in-line mass production. For in-line inspection, high-resolution non-destructive surface inspection techniques are required. Common surface inspection techniques include scanning electron microscopy (SEM), atomic force microscopy (AFM), optical microscopy (OM) and confocal differential interference contrast microscopy (CDIC), etc. For subsurface inspection, commonly used techniques include photoluminescence (PL), X-ray topography (XRT), mirror projection electron microscopy (MPJ), optical coherence tomography (OCT) and Raman spectroscopy, etc. In this review, we divide SiC inspection techniques into optical and non-optical methods and provide a discussion on each of techniques in the following sections.

Non-optical Defect Inspection Technologies

Non-optical inspection techniques, those not involving any kind of optical probing, such as KOH etching and TEM, have been widely used for characterizing the quality of SiC wafers. These methods are relatively mature and precise to inspect defects on SiC wafers. However, these methods cause irreversible damage to the samples which then are not suitable for the use in the production

lines. Although there exist other inspection methods like SEM, CL, AFM and MPJ which are non-destructive, the throughput of these methods is low and can serve as an assessment tool only. Next, we briefly introduce the principles of the above-mentioned non-optical technologies. Advantages and disadvantages of each individual technique are also brought under discussion.

Transmission Electron Microscopy (TEM)

The transmission electron microscopy (TEM) can be used to observe the subsurface structure of the sample at a nano-scale resolution. TEM makes use of accelerated electron beams incident onto the samples of SiC. Electrons with ultra-short wavelength and high energy pass through the surface of the sample which elastically scattered from the subsurface structure. Crystallographic defects in SiC, such as BPDs, TSDs and SFs, can be observed by using TEM [39–42].

A scanning transmission electron microscope (STEM) is a type of transmission electron microscope, which can obtain atomic-level resolution through high-angle annular dark-field imaging (HAADF). Images obtained through TEM and HAADF-STEM are shown in Fig. 4a. A trapezoidal SF and partial dislocations are clearly visualized by the TEM image while the HAADF-STEM images show three kind of SFs observed in 3C-SiC. These SFs consist of 1, 2, or 3 faulted atomic layers, indicated by the yellow arrows [43]. Though TEM is a useful defect inspection tool, it can only provide one cross-sectional view at a time, so it takes a lot of time if one needs to inspect whole SiC wafer. Besides, mechanism of the TEM demands that the sample must be very thin, with a thickness of less than 1 μm , which makes preparation of the sample quite complicated and time-consuming [44]. Overall, TEM is used to understand the fundamental crystallography of defects, but it is not a practical tool for large scale or in-line inspection.

KOH Etching

KOH etching is another non-optical technique used to inspect defects of several kinds, such as micropipes, TSDs, TEDs, BPDs and grain boundaries. The patterns formed after KOH etching depend on experimental conditions such as etching duration and temperature of the etchant. When molten KOH at about 500°C is added to SiC sample, it exhibits selective etching of SiC sample between areas with defects and those without defects in about 5 min [45]. After cooling and removing KOH from SiC sample, there are a lot of etched pits with different topography which are related to different types of defects. As shown in Fig. 4b, the dislocations produce large hexagonal etched pits assigned to micropipes, medium-sized pits to TSDs, and small-sized pits to TEDs. [45]

The advantage of KOH etching is that it can inspect all defects under the surface of SiC sample at one time, preparation of SiC sample is easy, and the cost is low. However, KOH etching is an irreversible process that can cause permanent damage to the sample. Further polishing of the sample is required to obtain a smooth surface after KOH etching.

Mirror Projection Electron Microscopy (MPJ)

Mirror projection electron microscopy (MPJ) is another promising subsurface inspection technique that allows the development of high throughput inspection systems capable of inspecting nanoscale defects. Since the MPJ reflects the equipotential image of surfaces on SiC wafers, the potential distortion caused by charged defects is distributed over a wider area than the actual defect size. Therefore, nanoscale defects can be inspected even the spatial resolution of the tool is in microscale. The electron beam from the electron gun passes through the focusing system and irradiates uniformly and normally onto the SiC wafer. Notably, the SiC wafer is irradiated by UV light, so the excited electrons are trapped by the defects present in the SiC wafer. Besides, SiC wafer is negatively charged to nearly equal to the acceleration voltage of the electron beam so that the incident electron beam decelerates and reflects before reaching the wafer surface. This phenomenon is similar to the reflection of light by a mirror, so the reflected electron beams are referred to as "mirror electrons." When the incident electron beam irradiates the SiC wafer carrying defects, the negatively charged state of the defect varies the equipotential surface, resulting in nonuniformity of the reflected electron beam. MPJ is a non-destructive inspection technique capable of imaging the static electrical potential topography on SiC wafers with high sensitivity. Isshiki et al. use MPJ to clearly identify BPDs, TSDs and TEDs after KOH etching [50]. Hasegawa et al. show images of BPDs, scratches, SFs, TSDs, and TEDs inspected by using MPJ [51] and discuss the relationship between latent scratches and step bunching [52].

Atomic Force Microscopy (AFM)

Atomic force microscopy (AFM) is generally applied to measure the surface roughness of SiC wafers with demonstrated resolution on atomic scale. The major difference between AFM and other surface inspection methods is that it does not suffer from diffraction limit of optical beams or aberration of lenses. AFM uses the interaction force between the probe tip on the cantilever and the surface of SiC wafer to measure the deflection of the cantilever which is then transduced into an electrical signal proportional to the characteristic appearance of the surface defects. AFM can form three-dimensional

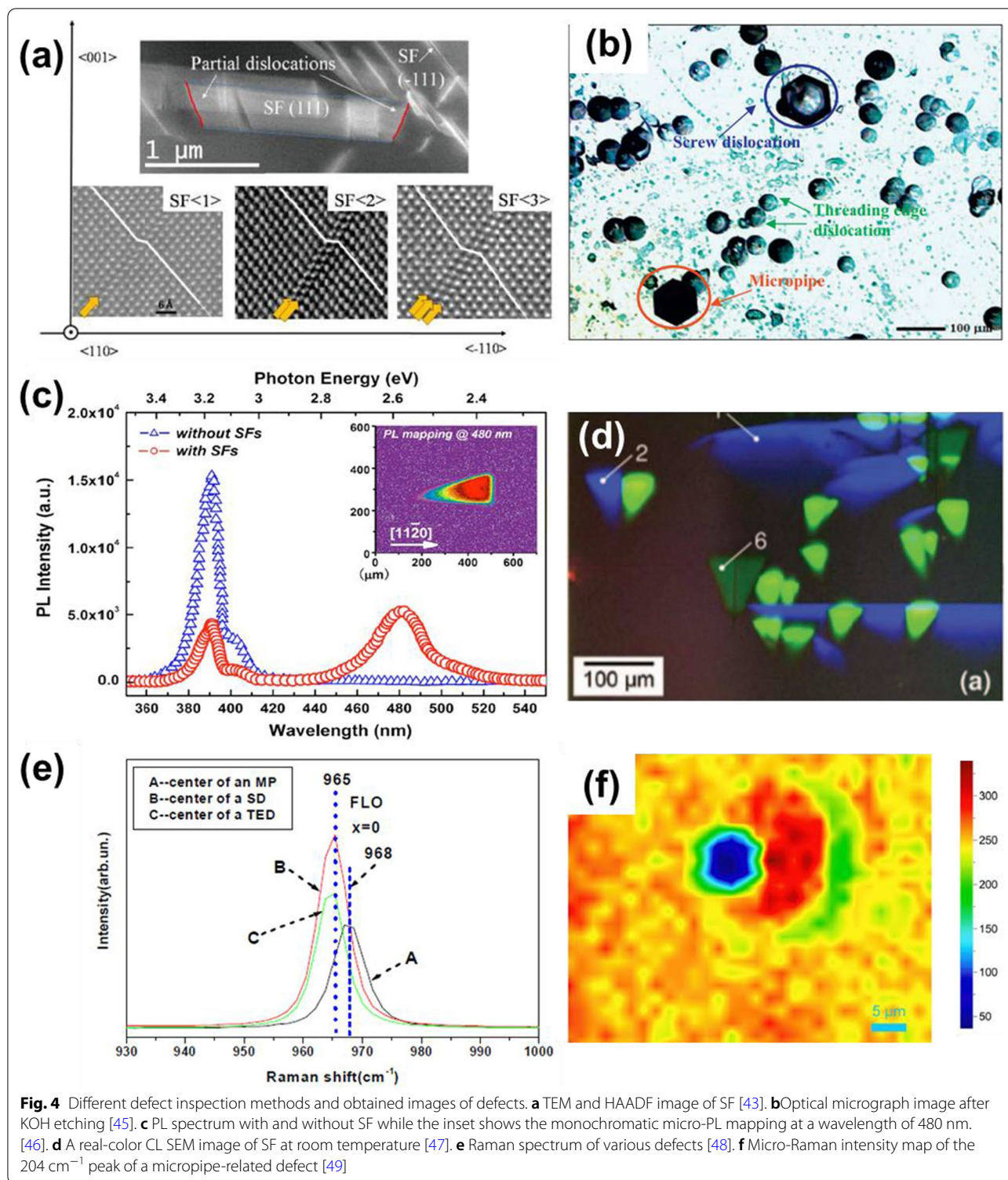


Fig. 4 Different defect inspection methods and obtained images of defects. **a** TEM and HAADF image of SF [43]. **b** Optical micrograph image after KOH etching [45]. **c** PL spectrum with and without SF while the inset shows the monochromatic micro-PL mapping at a wavelength of 480 nm. [46]. **d** A real-color CL SEM image of SF at room temperature [47]. **e** Raman spectrum of various defects [48]. **f** Micro-Raman intensity map of the 204 cm⁻¹ peak of a micropipe-related defect [49]

images of surface defects, but it is limited to resolve the topology of the surface and is time-consuming, so the throughput is low [53].

Scanning Electron Microscopy (SEM)

Scanning electron microscopy (SEM) is another non-optical technique used extensively for defect analysis of SiC wafers. SEM has high spatial resolution on the order

of nanometers. A focused electron beam generated by accelerator scans the surface of SiC wafer and interacts with SiC atoms to produce various types of signals such as secondary electrons, back-scattered electrons and X-rays. SEM images corresponding to the output signal show the characteristic appearance of surface defects, which is useful for understanding structural information of SiC crystals. However, SEM is limited to surface inspection only and does not provide any information on sub-surface defects.

Cathodoluminescence (CL)

Cathodoluminescence (CL) spectroscopy makes use of focused electron beams to probe electronic transitions in a solid which results in the emission of characteristic light. CL facility usually comes with SEM because an electron beam source is common feature of the two technologies. Accelerated electron beams strike the SiC wafer and produce excited electrons. The radiative recombination of excited electrons emits photons with wavelengths in the visible spectrum. By combining the structural information and the functional analysis, CL gives a full description of a sample with direct correlation of a sample's shape, size, crystallinity, or composition with its optical properties. Maximenko et al. show the all-color CL image of SFs at room temperature, as displayed in Fig. 4d [47]. Different kinds of SFs corresponding to different wavelengths are apparent, and a common single-layer Shockley-type stacking fault with a blue emission at ~ 422 nm and a TSD at ~ 540 nm is found by the CL [47]. Although SEM and CL have a high-resolution owing to the electron beam source, the high energy electron beam might cause damage to the surface of the sample.

Optical-Based Defect Inspection Technology

In pursuit of in-line mass production with high throughput without loss of inspection accuracy, optical-based inspection methods are promising because they can preserve the samples and most of them can provide rapid scanning capabilities. Surface inspection methods can be listed as OM, OCT and DIC, while Raman, XRT and PL are subsurface inspection methods. In this section, we describe the principles of each inspection method, how these apply in inspecting defects, and pros and cons of each method.

Optical Microscopy (OM)

The optical microscopy (OM), originally developed to closely view samples using light and optical magnifying components, can be utilized to inspect surface defects. This technique enables producing images in dark-field mode, bright-field mode, and phase mode, each giving specific defect information, and the combination of these

images provides the ability to identify most of the surface defects [54]. When the inspection light illuminates on the surface of the SiC wafer, the dark-field mode captures the scattered light by surface defects, so the image has a dark background that excludes the unscattered light as well as bright objects that indicates the location of defects. On the other hand, the bright-field mode captures the unscattered light, showing a white background image with dark objects due to scattering of defects. The phase mode captures the images with phase shift, which are accumulated by the contamination on the surface of the SiC wafer, showing a phase-contrast image. The scattering image of OM is advantageous in lateral resolution, while the phase-contrast image mainly aims at examining the smoothness of the wafer surface. Several studies have made efficient use of optical microscopy to characterize surface defects. Pei Ma et al. show that very thin carrot defects or micropipe defects are too small to be inspected by optical coherence tomography (OCT) but can be examined by optical microscopy due to its advantages in lateral resolution [33]. Zhao et al. use OM to study the origin of polytype inclusions, surface pits and step-bunching [34].

Optical Coherence Tomography (OCT)

Optical coherence tomography (OCT) is an optical inspection techniques that can provide rapid, nondestructive and 3D subsurface images of investigated samples. Since OCT was originally applied for the diagnosis of many diseases, most of its applications have been to resolve images of biological and clinical biomedical samples. However, there has been a growing interest in applying OCT for inspection of defects in SiC wafers since the resolution of OCT has been improved to a sub-micron scale due to the development of advanced optical components for visible and infrared wavelengths. The light source used in OCT has a broadband spectrum consisting of a wide range of frequencies in the visible and infrared region, so the coherence length is small, which means that the axial resolution can be very high, while the lateral resolution depends on functionality of the optics. The principle of OCT is based on low-coherence interferometry, which is typically a Michelson type setup. The source light of the OCT is divided into two arms, a reference arm and an inspection arm. The light beam to the reference arm is reflected by a mirror, while the light beam to the inspection arm is reflected by the SiC wafer. By moving the mirror in the reference arm, the combination of the two light beams gives rise to interference, but only if the optical path difference between the two beams is less than a coherence length. Therefore, the interference signal acquired by the detector contains cross-sectional information of the SiC wafer,

and by combining these cross-sectional inspections laterally, a 3D image of OCT can be achieved. However, the inspection speed and lateral resolution of OCT are still not comparable to other 2D inspection techniques, and the interference of surface scattering and absorption loss in the operating spectral range are the main limitations of OCT image formation. Pei Ma et al. use OCT to analyze carrot defects, polytype inclusions, grain boundaries and hexagonal voids [33]. Duncan et al. apply OCT to study the internal structure of single crystal SiC [55].

Differential Interference Contrast (DIC)

Differential interference contrast (DIC) is a microscopy technique that introduces phase contrast to the images of surface defects. The advantages of using DIC over OM are that the resolution of DIC is much higher than the phase mode of OM, because the image formation in DIC is not restricted by the aperture, and DIC can produce three-dimensional defect images by employing a confocal scanning system. The source light of DIC is linearly polarized by a polarizer and then split into two orthogonally polarized sub-beams, i.e., the reference beam and the inspection beam, by making it pass through a Wollaston prism. The reference beam strikes the normal surface of the SiC wafer, while the inspection beam strikes the surface of the SiC wafer with defects, producing a phase delay corresponding to the geometry of defects and alteration of optical path length. Since the two sub-beams are orthogonally polarized, they cannot interfere with each other during inspection until they are brought together after passing through a Wollaston prism again and enter an analyzer to generate defect-specific interference patterns. The processor then receives the defect signals to form a two-dimensional differential interference contrast image. To generate a three-dimensional image, a confocal scanning system can be used to shut off the two sub-beams that are offset from the focus of the system to avoid false inspections. Therefore, by making the focal point of the confocal system move in the direction of the optical axis, a three-dimensional defect image of the SiC wafer surface can be obtained. Sako et al. show that a surface defect with a scraper-shaped surface profile on the SiC epitaxial layer has been observed using CDIC. [56]. Kitabatake et al. establish the integrated evaluation platform using CDIC to inspect surface defects on the SiC wafers and the epitaxial films [57, 58].

X-Ray Diffraction Topography (XRT)

X-ray diffraction topography (XRT) is a powerful subsurface inspection technique that can help investigate the crystallographic structure of SiC wafers since the wavelength of X-rays is comparable with the distance between interatomic planes of SiC crystal. It is used to evaluate

the structural characteristics of SiC wafers by measuring the change in diffraction intensity due to the strain field caused by defects. This means that crystallographic defects cause a change in lattice spacing or lattice rotation around them, forming a strain field. XRT is commonly used in production line with high throughput and sufficient resolution; however, it requires a large-scale apparatus for emission of X-rays and its defect mapping capabilities still require improvement. The image formation mechanism of XRT is based on Laue condition (momentum conservation), where a collimated beam of X-rays is produced when the electron beam generated by a heated filament is collimated and accelerated by a high electric potential to obtain sufficient energy, which is then directed to the metal anode. When X-rays are irradiated onto a SiC wafer, a unique diffraction pattern with several narrow and sharp peaks is formed and inspected by the detector due to the constructive and destructive interference of X-rays scattered at specific angles from the interatomic planes of SiC. Thus, crystallographic defects can be characterized by diffraction peak broadening analysis, where the diffraction spectrum is narrow and sharp if no defects are present; otherwise, the spectrum is broadened or shifted if there is a defect-induced strain field. The detection mechanism of XRT is based on X-rays diffraction rather than electrons scattering, thus classifying XRT as an optical technique while SEM is a non-optical technique. Chikvaidze et al. use XRT to confirm defects with different stacking sequence in the SiC sample [59]. Senzaki et al. show the transformation of extended BPDs to TED is origins of triangular-shaped single Shockley-type stacking fault (1SSF) inspected using XRT under current stress test [60]. Current in-line XRT is typically used to identify the defect structure without recognizable inspection signal from other inspection techniques such as PL and OM.

Photoluminescence (PL)

Photoluminescence (PL) is one of the most common subsurface inspection technique being used to inspect crystallographic defects. The high throughput of PL makes it suitable for in-line mass production. SiC is an indirect bandgap semiconductor that shows PL at near band-edge emission of about 380 nm wavelength. Recombination at through defect level in SiC wafers could be radiative. UV excitation-based PL technique has been developed to identify defects present inside SiC wafers, such as BPDs and SFs [61]. However, defects without characteristic PL features or with weak PL contrast against defect-free SiC region, such as scratches and threading dislocations, should be evaluated by other inspection methods. Since emission energy varies depending on the trap levels of defects, PL images with spectral resolution could be used

to differentiate each type of defects and map them [15]. The PL spectrum of polytype SF exhibits multi-peak spectra in the wavelength range of 350–550 nm due to the quantum-well-like band structure induced by SFs. Each type of SF can be distinguished by examining their emission spectra using bandpass filter that filters out individual spectra, as shown in Fig. 4c [15, 46]. Berwian et al. construct a defect luminescence scanner based on UV-PL to clearly inspect BPDs, SFs and polytype inclusions [62]. Tajima et al. use PL with a variety of excitation wavelengths ranging from deep UV to visible and NIR to inspect TEDs, TSDs, SFs and examine the correlation between the PL and etched pit patterns [63]. Nevertheless, the PL images of some defects are similar, such as BPDs and carrot defects, which both show line-shaped features, making it difficult for PL to distinguish between them, so other structural analysis tools, such as XRT or Raman spectroscopy, are often used in parallel with PL to accurately classify these defects.

Raman Spectroscopy

Raman spectroscopy has a wide variety of applications in biology, chemistry and nanotechnology to identify features of molecules, chemical bonds and nanostructures. Raman spectroscopy is a non-destructive sub-surface inspection method that can verify different crystalline structures and crystallographic defects in SiC wafers [64, 65]. Typically, the SiC wafer is irradiated by a laser and the laser light interacts with molecular vibrations or phonons in the SiC that puts the molecule into a virtual energy state, resulting in an upward or downward shift in the wavelength of the inspected photons, referred to as Stokes Raman scattering or Anti-Stokes Raman scattering, respectively. The shift in the wavelength gives information about the vibrational modes in

SiC, corresponding to the different polytype structures. It has been shown that the characteristic peaks at 200 and 780 cm^{-1} in the measured Raman spectrum indicate the 4H-polytype of SiC, while the characteristic peaks at 160, 700 and 780 cm^{-1} represent the 6H-polytype of SiC [66]. Chikvaidze et al. use Raman spectroscopy to confirm a 2H-SiC polytype with Raman peaks around 796 and 971 cm^{-1} present in the 3C-SiC sample [67]. Hundhausen et al. use Raman spectroscopy to study the polytype conversion of 3C-SiC during high-temperature annealing [68]. Feng et al. find the peak center shift and the intensity variation of micropipes, TSDs and TEDs, as shown in Fig. 4e [48]. For spatial information, an image of Raman mapping is shown in Fig. 4f [49]. Generally, the Raman scattering signal is very weak, so it takes a long time for Raman spectroscopy to collect sufficient signal. The technique could be used for detail analysis of the defect physics, but it is not suitable for in-line inspection due to weak signal and current technology limits.

The types of defects that can be inspected by the inspection methods discussed in this paper and their corresponding researches are summarized in Table 3, which still requires more research data to be completed.

Impact of Defects on Devices

Each type of defect adversely affects the quality of the wafer and deteriorates the devices subsequently fabricated on it. The deterioration between defects and device failures is related to the kill ratio, which defined as the proportion of defects estimated to cause device failure. The kill ratio for each defect type varies depending on the end application. Specifically, those defects that cause significant impact on the device are referred to as killer defects [88]. Previous studies have shown the correlation between defects and device

Table 3 Research on various inspection methods and inspected defect types

	Non-optical						Optical				
	Inspection			Metrology			Inspection		Metrology		
	KOH	SEM	AFM	TEM	CL	MPJ	OCT	DIC	XRT	PL	Raman
<i>Crystal defect</i>											
Micropipe	[45]	[16]	[69]	[70]	[71]	X	O	O	[72]	[15]	[48]
TSD/TED	[45, 46, 73]	[73]	O	[74]	[47]	[51, 73]	O	O	[16, 75]	[15, 61, 76]	[48]
BPD	[46, 73]	X	X	[74]	[77]	[51, 73]	X	X	[75]	[15, 61]	O
SF	[78]	[16]	O	[43, 46, 74]	[47]	[51]	O	O	[76]	[15, 61, 46]	[17]
<i>Surface defect</i>											
Scratch		[79]	[79]		O	[51, 79]	O	O	[15, 80]	X	[17]
Carrot		[16]	O		[81]	[82]	[33]	[82]	[83]	[15]	O
Triangular		[16]	[25]		[71]	O	[33]	[84]	[84]	[85]	[84–86]
Downfall		[87]	O		[87]	X	O	O	X	X	O

performance [89, 90]. We discuss the impact of different defects on different devices in this section.

In MOSFET, BPDs increase on-resistance [91] and reduce the gate oxide reliability [92]. Micropipes limit the operation current and increase the leakage current [93, 94] while defects such as SFs, carrots and polytype inclusions reduce blocking voltage [4, 91] and scratches on the surface cause reliability issues [95]. Isshiki et al. show that there are latent scratches, consisting of complex stacking faults and dislocation loops lying beneath the SiC substrate, resulting in formation of step bunching and degradation of dielectric strength of oxide film in SiC-MOSFETs [79]. Other surface defects such as trapezoidal features might lead to significant impact on the channel mobility or the oxide breakdown characteristics in SiC MOSFETs [96].

In Schottky barrier diode, BPDs, TSDs and TEDs increase the reverse leakage current [97–101] while micropipes and SFs reduce the blocking voltage [85, 89, 102]. Carrots and polytype inclusions both reduce blocking voltage and increase leakage current while scratches cause barrier height inhomogeneity [103].

In a p - n diode, BPDs increase the on-resistance and leakage current [91] while TSDs and TEDs reduce blocking voltage [104]. Micropipes limit the operation current and increase the leakage current [93, 94] while SFs increase forward voltage [105]. Carrots and polytype inclusions reduce blocking voltage and increase leakage current [72, 106] while scratches on the surface have no direct impact on p - n diode. Skowronski et al. show that during the diode operation, the BPD within the SiC epitaxial layer is transformed into a SFs or allows the SFs to extend along the BPD through electrical conduction, resulting in current degradation that increases the resistance of the SiC p - n diode [60]. Studies have also proved that the SFs may give rise to a 3C-SiC polytype, resulting in decrease in minority carrier lifetime of the SiC p - n diode because the 3C-SiC polytype has a lower bandgap than the 4H-SiC polytype, so a SF act as a quantum well that enhances the recombination rate [107]. Moreover, the single Shockley-type SFs are expanded under PL characterization, causing a change in junction potential which in turn deteriorates the on-resistance of SiC p - n diode [108]. Furthermore, TSDs result in degradation of the blocking voltage and TEDs reduce the minority carrier lifetime of the SiC p - n diode [109].

In bipolar devices, BPDs reduce the gate oxide reliability [51, 110] while TSDs and TEDs reduce carrier lifetime [111]. Micropipes limit the operation current [94] while SFs reduce carrier lifetime [111]. Carrots and polytype inclusions reduce blocking voltage and increase leakage current and reduce carrier lifetime [84, 112].

Point defects (vacancies) in SiC reduce the carrier lifetime of the device [24], leading to junction leakage currents [113] and resulting in lower breakdown voltages. Although point defects have a negative impact on electronic devices, they find some useful applications as well, such as in quantum computing [114, 115]. Lukin et al. show that point defects in SiC such as silicon vacancy and carbon vacancy can produce stable bound states with suitable spin-orbit attributes, serving as hardware platform choices for quantum computation [116].

The impacts of defects on different devices are organized in Fig. 5. As one can see, defects can deteriorate the device characteristics in many ways [91, 117]. Although the negative effects of defects can be counteracted by designing different device structures [1–3, 118–123], establishing a fast and accurate defect inspection system is amid a pressing need to help one observe defects and further optimize the process to reduce them. Note that analyzing the characteristics of SiC devices to identify type and the presence of defects could potentially be used as a defect inspection method (Figs. 6 and 7).

An efficient defect inspection system requires the ability to identify surface defects and crystallographic defects simultaneously, put all defects to the correct category and then display the mapping of defects distribution data of the entire wafer by using multi-channel machine learning algorithms. Kawata et al. design an automatic inspection algorithm for the dislocation contrasts of n -type SiC wafers in a birefringence image and succeed in inspecting the position of the dislocation contrasts of XRT images with relatively high precision and sensitivity [124]. Leonard et al. use deep convolutional neural network (DCNN) machine learning for automated defect inspection and classification by using PL images of unetched wafers coupled with automatically labelled images of the corresponding etched wafers as the training set. The defect locations and classifications determined by DCNN correlate well with the subsequently etch delineated features [125]. Monno et al. propose a deep learning system which inspecting defects on SiC substrate by SEM and classifying them with a 70% accuracy. The proposed approach can combine multiple tiles without inconsistency of linear defects and can inspect and classify the seven defects, with a very good degree of accuracy [126, 127].

Apart from inspecting defects, reducing their density is also a useful approach to improve the quality and the yield of SiC devices. By using micropipe-free seeds or a solution-based growth, the density of micropipe and TSDs can be decreased [112, 128]. To reduce the surface defects caused by mechanical processes, some studies point out that femtosecond lasers can be used to improve the efficiency of chemical-mechanical planarization [129] and the cutting quality [67, 130–133]. Femtosecond

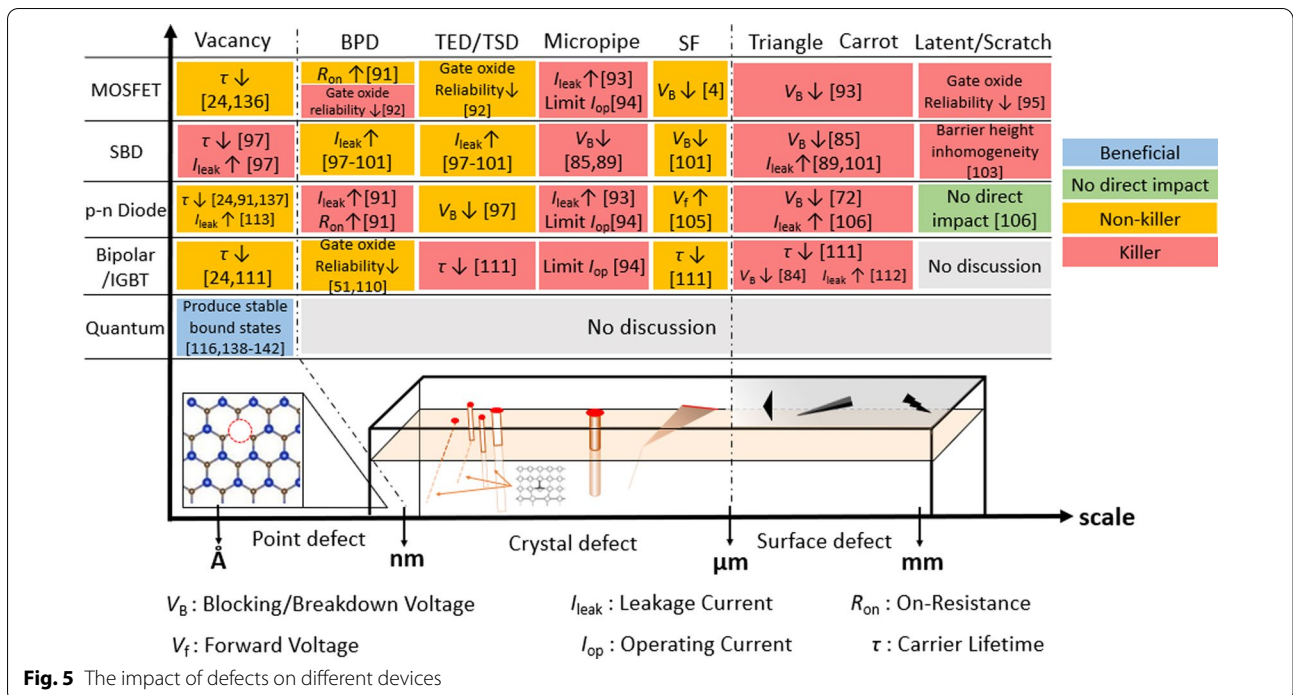


Fig. 5 The impact of defects on different devices

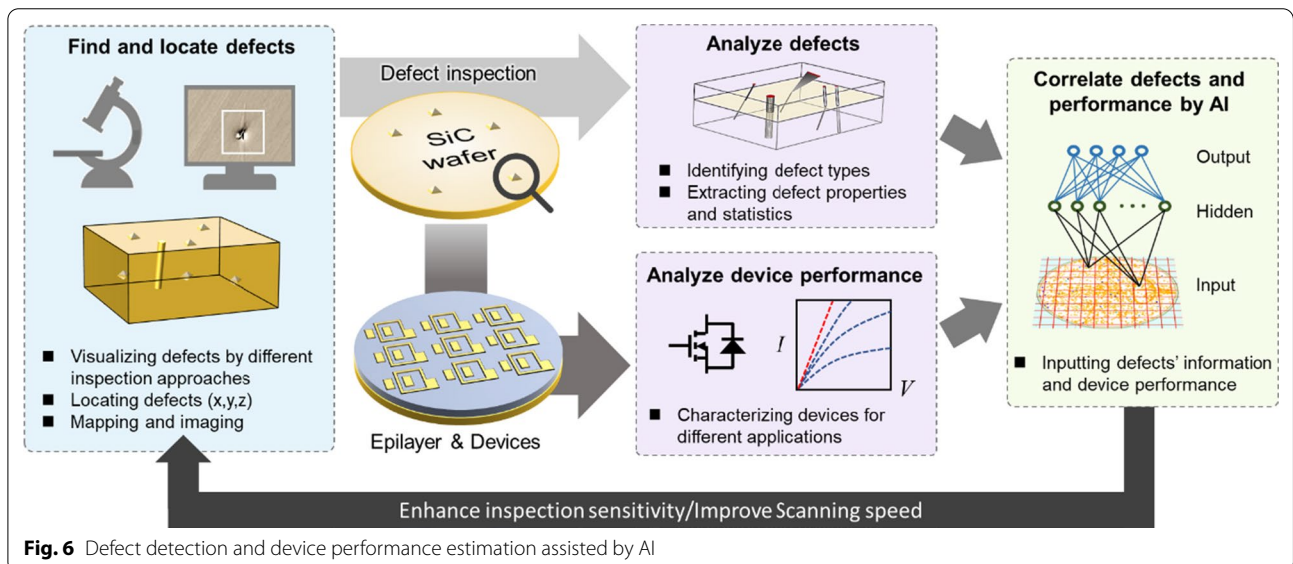
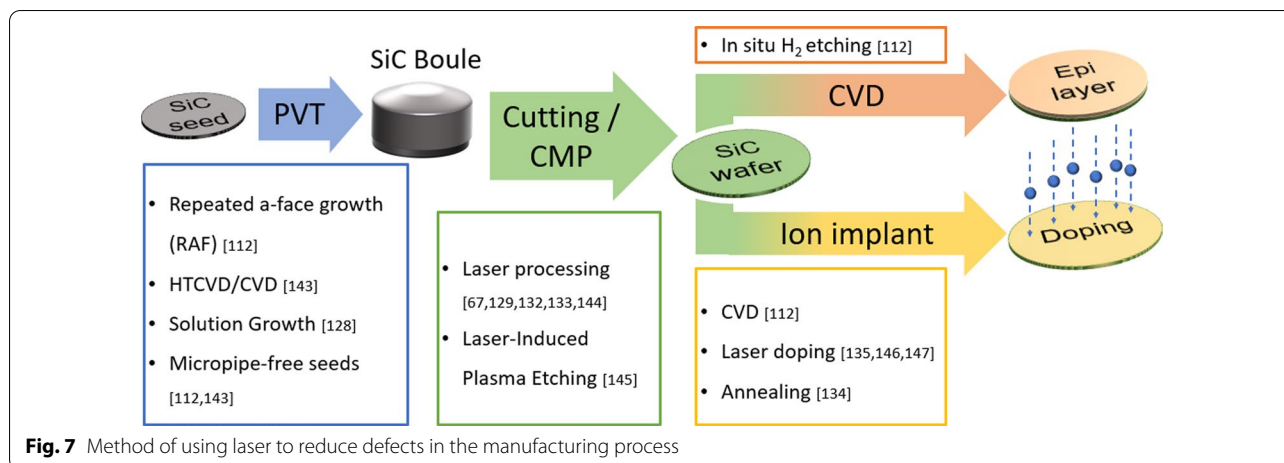


Fig. 6 Defect detection and device performance estimation assisted by AI



laser annealing can also improve the quality of ohmic contact between Ni and SiC and increase the conductivity of the device [134]. In addition to the application of femtosecond lasers, some other teams also found that the use of laser-induced liquid phase doping (LILPD) can effectively reduce the damage generated during the process [135].

Conclusion

In this review article, we described the importance of defect inspection in the SiC industry, especially of those known as killer defects. Details of the crystallographic and surface defects that often arise during the production of SiC wafers as well as the nature of deterioration caused by these defects in different devices are comprehensively reviewed. Surface defects are detrimental to most devices, while crystallographic defects are risky for defect transformation and wafer quality. After understanding the impact of defects, we summarize the principles of common surface and subsurface inspection techniques, how these are applied in inspecting defects, and pros and cons of each method. The destructive inspection techniques can provide observable, reliable, and quantitative information; however, these cannot meet the requirements of in-line mass production since these are time consuming and adversely affect the quality of sample. On the other hand, non-destructive inspection techniques, especially optical-based techniques, are more applicable and efficient in production line. Note that different inspection techniques are complementary to each other. A combinational use of inspection techniques could potentially balance the tradeoff between throughput, resolution and equipment complexity. In the future, it is anticipated that non-destructive inspection methods with high-resolution and rapid scanning capabilities are integrated into the perfect defect inspection systems

capable of simultaneously inspecting surface defects and crystallographic defects, then using multi-channel machine learning algorithms to assign all defects to the correct category and display the mapping image of defect distribution data to the entire SiC wafer.

Abbreviations

SiC: Silicon carbide; Si: Silicon; GaAs: Gallium arsenide; GaN: Gallium nitride; MOSFET: Metal-oxide-semiconductor field-effect transistor; SBD: Schottky barrier diode; IGBT: Insulated gate bipolar transistor; PVT: Physical vapor transport; CMP: Chemical-mechanical planarization; CVD: Chemical vapor deposition; Epi layer: Epitaxial layer; KOH: Potassium hydroxide; TEM: Transmission electron microscopy; STEM: Scanning transmission electron microscope; HAADF: High-angle annular dark-field imaging; SEM: Scanning electron microscopy; AFM: Atomic force microscopy; XRT: X-ray topography; XRD: X-ray diffraction; Raman: Raman spectroscopy; PL: Photoluminescence; MPJ: Mirror projection electron microscopy; OCT: Optical coherence tomography; OM: Optical microscopy; CL: Cathodoluminescence; DIC: Differential interference contrast; C-DIC: Confocal differential interference contrast microscopy; BPD: Basal plan dislocation; SF: Stacking faults; TED: Threading edge dislocation; TSD: Threading screw dislocation; APDs: Anti-phase domains; BSDs: Black spot defects; DCNN: Deep convolutional neural network; LILPD: Laser-induced liquid phase doping; HTCVD: High-temperature chemical vapor deposition.

Acknowledgements

Authors gratefully acknowledge the financial supported by Ministry of Science and Technology, Taiwan (Grant No. MOST 110-2112-M-009-010-MY3). This work was supported by the Higher Education Sprout Project of the National Yang Ming Chiao Tung University and Ministry of Education (MOE), Taiwan. D.H.L. acknowledges the Yushan Scholar Program supported by the Ministry of Education, Taiwan.

Authors' Contributions

Data curation was contributed by P-CC, W-CM; supervision was contributed by S-CC, D-HL and H-CK; writing—original draft, was contributed by P-CC, W-CM, TA; review and editing were contributed by B-YT, D-HL. All authors have read and agreed to the published version of the manuscript.

Funding

Not applicable.

Availability of Data and Materials

Not applicable.

Declarations

Competing interests

The authors declare no competing interests.

Author details

¹Institute of Electronics, College of Electrical and Computer Engineering, National Yang Ming Chiao Tung University, Hsinchu 30010, Taiwan. ²Semiconductor Research Center, Hon Hai Research Institute, Taipei 11492, Taiwan. ³Department of Photonics and Institute of Electro-Optical Engineering, College of Electrical and Computer Engineering, National Yang Ming Chiao Tung University, Hsinchu 30010, Taiwan. ⁴Department of Electrophysics, College of Science, National Yang Ming Chiao Tung University, Hsinchu 30010, Taiwan.

Received: 24 December 2021 Accepted: 16 February 2022

Published online: 04 March 2022

References

- Matallana A, Robles E, Ibarra E, Andreu J, Delmonte N, Cova P (2019) A methodology to determine reliability issues in automotive SiC power modules combining 1D and 3D thermal simulations under driving cycle profiles. *Microelectron Reliab* 102:113500
- Monteverde F, Scatteia L (2007) Resistance to thermal shock and to oxidation of metal diborides–SiC ceramics for aerospace application. *J Am Ceram Soc* 90(4):1130–1138
- Kadavelugu A, Bhattacharya S, Ryu SH, Van Brunt E, Grider D, Agarwal A, Leslie S (2013) Characterization of 15 kV SiC n-IGBT and its application considerations for high power converters. In: 2013 IEEE energy conversion congress and exposition. IEEE, pp 2528–2535
- Kimoto T (2015) Material science and device physics in SiC technology for high-voltage power devices. *Jpn J Appl Phys* 54(4):040103
- Kaminski N, Hilt O (2014) SiC and GaN devices-wide bandgap is not all the same. *IET Circuits Devices Syst* 8(3):227–236
- Sugawara Y, Takayama D, Asano K, Singh R, Palmour J, Hayashi T (2001) 12–19 kV 4H-SiC pin diodes with low power loss. In: Proceedings of the 13th international symposium on power semiconductor devices & ICs. IPD'01 (IEEE Cat. No. 01CH37216). IEEE, pp 27–30
- Henry A, ul Hassan J, Bergman JP, Hallin C, Janzen E (2006) Thick silicon carbide homoepitaxial layers grown by CVD techniques. *Chem Vap Depos* 12(8–9):475–482
- Ding X, Du M, Zhou T, Guo H, Zhang C (2017) Comprehensive comparison between silicon carbide MOSFETs and silicon IGBTs based traction systems for electric vehicles. *Appl Energy* 194:626–634
- Bhatnagar M, McLarty PK, Baliga BJ (1992) Silicon-carbide high-voltage (400 V) Schottky Barrier diodes. *IEEE Electron Device Lett* 13(10):501–503
- Yoder MN (1996) Wide bandgap semiconductor materials and devices. *IEEE Trans Electron Devices* 43(10):1633–1636
- Hudgins JL, Simin GS, Santi E, Khan MA (2003) An assessment of wide bandgap semiconductors for power devices. *IEEE Trans Power Electron* 18(3):907–914
- Zetterling CM (ed) (2002) Process technology for silicon carbide devices (No. 2). IET, London
- Kurita T, Miyake K, Kawata K, Ashida K, Kato T (2016) Development of new complex machining technology for single crystal silicon carbide polishing. *Int J Autom Technol* 10(5):786–793
- Song H, Sudarshan TS (2013) Basal plane dislocation conversion near the epilayer/substrate interface in epitaxial growth of 4 off-axis 4H–SiC. *J Cryst Growth* 371:94–101
- Non-destructive recognition procedures of defects in silicon carbide wafers: Parts 1–3. JEITA Standards, EDR-4712/100/200/300, (2016–2018)
- Matsuhata H, Sugiyama N, Chen B, Yamashita T, Hatakeyama T, Sekiguchi T (2017) Surface defects generated by intrinsic origins on 4H-SiC epitaxial wafers observed by scanning electron microscopy. *Microscopy* 66(2):95–102
- Nakashima SI, Mitani T, Tomobe M, Kato T, Okumura H (2016) Raman characterization of damaged layers of 4H-SiC induced by scratching. *AIP Adv* 6(1):015207
- Tsuchida H, Kamata I, Izumi S, Tawara T, Izumi K (2004) Growth and characterization of the 4H-SiC epilayers on substrates with different off-cut directions. In: Materials science forum, vol 457. Trans Tech Publications Ltd, pp 229–232
- Shrivastava A, Muzykov P, Caldwell JD, Sudarshan TS (2008) Study of triangular defects and inverted pyramids in 4H-SiC 4° off-cut (0 0 0 1) Si face epilayers. *J Cryst Growth* 310(20):4443–4450
- Benamara M, Zhang X, Skowronski M, Ruterana P, Nouet G, Sumakeris JJ, Paisley MJ, O'Loughlin MJ (2005) Structure of the carrot defect in 4H-SiC epitaxial layers. *Appl Phys Lett* 86(2):021905
- Feng G, Suda J, Kimoto T (2008) Characterization of stacking faults in 4 H-Si C epilayers by room-temperature microphotoluminescence mapping. *Appl Phys Lett* 92(22):221
- Son NT, Zolnai Z, Janzén E (2003) Silicon vacancy related T V 2 a center in 4H-SiC. *Phys Rev B* 68(20):205211
- Orlinski SB, Schmidt J, Mokhov EN, Baranov PG (2003) Silicon and carbon vacancies in neutron-irradiated SiC: a high-field electron paramagnetic resonance study. *Phys Rev B* 67(12):125207
- Kalinina EV (2007) The effect of irradiation on the properties of SiC and devices based on this compound. *Semiconductors* 41(7):745–783
- Ohtani N (2011) Toward the reduction of performance-limiting defects in SiC epitaxial substrates. *ECS Trans* 41(8):253
- Kamei K, Kusunoki K, Yashiro N, Okada N, Tanaka T, Yuchi A (2009) Solution growth of single crystalline 6H, 4H-SiC using Si–Ti–C melt. *J Cryst Growth* 311(3):855–858
- Kubota T, Talekar P, Ma X, Sudarshan TS (2005) A nondestructive automated defect detection system for silicon carbide wafers. *Mach Vis Appl* 16(3):170–176
- Cheung R (2006) Silicon carbide microelectromechanical systems for harsh environments. World Scientific, Singapore
- Feng G, Suda J, Kimoto T (2009) Characterization of major in-grown stacking faults in 4H-SiC epilayers. *Physica B Condens Matter* 404(23–24):4745–4748
- Hong MH, Samant AV, Pirouz P (2000) Stacking fault energy of 6H-SiC and 4H-SiC single crystals. *Philos Mag A* 80(4):919–935
- Guziewski M, Montes de Oca Zapiaín D, Dingreville R, Coleman SP (2021) Microscopic and macroscopic characterization of grain boundary energy and strength in silicon carbide via machine-learning techniques. *ACS Appl Mater Interfaces* 13(2):3311–3324
- Wutimakun P, Buteprongjit C, Morimoto J (2009) Nondestructive three-dimensional observation of defects in semi-insulating 6H-SiC single-crystal wafers using a scanning laser microscope (SLM) and infrared light-scattering tomography (IR-LST). *J Cryst Growth* 311(14):3781–3786
- Ma P, Ni J, Sun J, Zhang X, Li J, Chen H (2020) Three-dimensional detection and quantification of defects in SiC by optical coherence tomography. *Appl Opt* 59(6):1746–1755
- Zhao L (2020) Surface defects in 4H-SiC homoepitaxial layers. *Nano-technol Precis Eng* 3(4):229–234
- Kimoto T (2016) Bulk and epitaxial growth of silicon carbide. *Prog Cryst Growth Charact Mater* 62(2):329–351
- Fujiwara H, Danno K, Kimoto T, Tojo T, Matsunami H (2005) Effects of C/Si ratio in fast epitaxial growth of 4H–SiC (0 0 0 1) by vertical hot-wall chemical vapor deposition. *J Cryst Growth* 281(2–4):370–376
- Hatakeyama T, Ichinoseki K, Fukuda K, Higuchi N, Arai K (2008) Evaluation of the quality of commercial silicon carbide wafers by an optical non-destructive inspection technique. *J Cryst Growth* 310(5):988–992
- Sakwe SA, Müller R, Wellmann PJ (2006) Optimization of KOH etching parameters for quantitative defect recognition in n- and p-type doped SiC. *J Cryst Growth* 289(2):520–526
- Liu C, He L, Zhai Y, Tyburska-Püschel B, Voyles PM, Sridharan K, Szlufarska I (2017) Evolution of small defect clusters in ion-irradiated 3C-SiC: combined cluster dynamics modeling and experimental study. *Acta Mater* 125:377–389
- La Via F, Severino A, Anzalone R, Bongiorno C, Litrico G, Mauceri M, Schoeler M, Schuh P, Wellmann P (2018) From thin film to bulk 3C-SiC growth: understanding the mechanism of defects reduction. *Mater Sci Semicond Process* 78:57–68
- Severino A, Frewin C, Bongiorno C, Anzalone R, Sadow SE, La Via F (2009) Structural defects in (100) 3C-SiC heteroepitaxy: influence of the buffer layer morphology on generation and propagation of stacking faults and microtwins. *Diamond Relat Mater* 18(12):1440–1449

42. Wu HZ, Roberts SG, Möbus G, Inkson BJ (2003) Subsurface damage analysis by TEM and 3D FIB crack mapping in alumina and alumina/5vol.% SiC nanocomposites. *Acta Mater* 51(1):149–163
43. Zimbone M, Sarikov A, Bongiorno C, Marzegalli A, Scuderi V, Calabretta C, Miglio L, La Via F (2021) Extended defects in 3C-SiC: stacking faults, threading partial dislocations, and inverted domain boundaries. *Acta Mater* 213:116915
44. Hristu R, Stanciu SG, Tranca DE, Matei A, Stanciu GA (2014) Nonlinear optical imaging of defects in cubic silicon carbide epilayers. *Sci Rep* 4(1):1–6
45. Mahajan S, Rokade MV, Ali ST, Rao KS, Munirathnam NR, Prakash TL, Amalnerkar DP (2013) Investigation of micropipe and defects in molten KOH etching of 6H n-silicon carbide (SiC) single crystal. *Mater Lett* 101:72–75
46. Feng G, Suda J, Kimoto T (2009) Triple Shockley type stacking faults in 4 H-SiC epilayers. *Appl Phys Lett* 94(9):091910
47. Maximenko SI, Freitas JA Jr, Klein PB, Shrivastava A, Sudarshan TS (2009) Cathodoluminescence study of the properties of stacking faults in 4 H-SiC homoepitaxial layers. *Appl Phys Lett* 94(9):092101
48. Feng X, Zang Y (2016) Raman scattering properties of structural defects in SiC. In: 2016 3rd international conference on mechatronics and information technology. Atlantis Press
49. Yang J, Song H, Jian J, Wang W, Chen X (2021) Characterization of morphological defects related to micropipes in 4H-SiC thick homoepitaxial layers. *J Cryst Growth* 568:126182
50. Isshiki T, Hasegawa M (2014). Non destructive inspection of dislocations in SiC wafer by mirror projection electron microscopy. In: *Materials science forum*, vol 778. Trans Tech Publications Ltd, pp 402–406
51. Hasegawa M, Kobayashi K (2019) Mirror electron inspection system Mirelis VM1000 for enhanced reliability of mobility systems. *Hitachi Rev* 68(1):115–120
52. Hasegawa M, Ohira K, Kaneoka N, Ogata T, Onuki K, Kobayashi K, Osanai T, Masumoto K, Senzaki J (2020) 4H-SiC Epi-ready substrate qualification by using mirror electron microscope inspection system. In: *Materials science forum*, vol 1004. Trans Tech Publications Ltd, pp 369–375
53. Steckl AJ, Roth MD, Powell JA, Larkin DJ (1993) Atomic probe microscopy of 3C SiC films grown on 6H SiC substrates. *Appl Phys Lett* 62:2545–2547
54. Candela Defect Inspectors | GaN SiC Wafer Inspection—KLA. <https://www.kla-tencor.com/products/instruments/defect-inspectors>. Accessed 29 Oct 2021
55. Duncan MD, Bashkansky M, Reintjes J (1998) Subsurface defect detection in materials using optical coherence tomography. *Opt Express* 2(13):540–545
56. Sako H, Yamashita T, Sugiyama N, Sameshima J, Ishiyama O, Tamura K, Senzaki J, Matsuhata H, Kitabatake M, Okumura H (2014) Characterization of scraper-shaped defects on 4H-SiC epitaxial film surfaces. *Jpn J Appl Phys* 53(5):0511301
57. Kitabatake M, Sameshima J, Ishiyama O, Tamura K, Oshima H, Sugiyama N, Yamashita T, Tanaka T, Senzaki J, Matsuhata H (2013) The integrated evaluation platform for SiC wafers and epitaxial films. *Mater Sci Forum* 740–742:451–454
58. Kitabatake M, Sako H, Sasaki M, Yamashita T, Tamura K, Yamada K, Ishiyama O, Senzaki J, Matsuhata H (2014) Electrical characteristics/reliability affected by defects analyzed by the integrated evaluation platform for SiC epitaxial films. In: *Materials science forum*, vol. 778–780, pp 979–984
59. Chikvaizde G, Mironova-Ulmane N, Plaupe A, Sergeev O (2014) Investigation of silicon carbide polytypes by Raman spectroscopy. *Latv J Phys Tech Sci* 51:51–57
60. Skowronski M, Ha S (2006) Degradation of hexagonal silicon-carbide based bipolar devices. *J Appl Phys* 99:011101
61. Oppel S, Schneider A, Schütz M, Kaminzky D, Kallinger B, Weber J, Krieger M. Defect luminescence scanner: scientific and industrial-scale defect analysis.
62. Berwian P, Kaminzky D, Rosshirt K, Kallinger B, Friedrich J, Oppel S, Schneider A, Schütz M (2016) Imaging defect luminescence of 4H-SiC by ultraviolet-photoluminescence. In: *Solid state phenomena*, vol 242. Trans Tech Publications Ltd, pp 484–489
63. Tajima M, Higashi E, Hayashi T, Kinoshita H, Shiomi H (2006) Characterization of SiC wafers by photoluminescence mapping. In: *Materials science forum*, vol 527. Trans Tech Publications Ltd, pp 711–716
64. Tseng YC, Cheng YC, Lee YC, Ma DL, Yu BY, Lin BC, Chen HL (2016) Using visible laser-based raman spectroscopy to identify the surface polarity of silicon carbide. *J Phys Chem C* 120(32):18228–18234
65. McCreery RL (2001) Raman spectroscopy for chemical analysis. *Meas Sci Technol* 12(5):653
66. Feng M, Wang YF, Hao JM, Lan GX (2003) Raman study of SiC polytype structure. *Chin J Light Scatter* 15:158–161
67. Liu C, Zhang X, Wang G, Wang Z, Gao L (2021) New ablation evolution behaviors in micro-hole drilling of 2.5 D Cf/SiC composites with millisecond laser. *Ceram Int* 47(21):29670–29680
68. Hundhausen M, Püsche R, Röhrl J, Ley L (2008) Characterization of defects in silicon carbide by Raman spectroscopy. *Physica Status Solidi (b)* 245(7):1356–1368
69. Ying-Xin C, Xiao-Bo H, Xian-Gang X (2018) As-grown Surface Morphologies of SiC Single Crystals Grown by PVT Method. *J Inorg Mater* 33(8):877–882
70. Scholz R, Gösele U, Wischmeyer F, Niemann E (1998) Prevention of micropipes and voids at β -SiC/Si (100) interfaces. *Appl Phys A Mater Sci Process* 66(1):59–67
71. MacMillan MF, Hultman L, Ivanov IG, Janzen E, Hallin C, Henry A, Galloy SA (1998) Cathodoluminescence of defect regions in SiC epi-films. In: *Materials science forum*, vol 264
72. Kohn VG, Argunova TS, Je JH (2007) Study of micropipe structure in SiC by x-ray phase contrast imaging. *Appl Phys Lett* 91(17):171901
73. Isshiki T, Hasegawa M (2015) Study on formation of dislocation contrast in 4H-SiC wafer in mirror projection electron microscopy image. In: *Materials science forum*, vol 821. Trans Tech Publications Ltd, pp 307–310
74. Konishi K, Yamamoto S, Nakata S, Nakamura Y, Nakanishi Y, Tanaka T, Tomita N, Yamakawa S (2013) Stacking fault expansion from basal plane dislocations converted into threading edge dislocations in 4H-SiC epilayers under high current stress. *J Appl Phys* 114(1):014504
75. Peng H, Liu Y, Ailihumaer T, Raghothamachar B, Dudley M, Sampayan K, Sampayan S (2021) Investigation of dislocations in 6H-SiC axial samples using synchrotron X-ray topography and ray tracing simulation. *ECS Trans* 104(7):147
76. Tanaka A, Matsuhata H, Kawabata N, Mori D, Inoue K, Ryo M, Fujimoto T, Tawara T, Miyazato M, Miyajima M, Kimoto T (2016) Growth of Shockley type stacking faults upon forward degradation in 4H-SiC pin diodes. *J Appl Phys* 119(9):095
77. Hidalgo P, Ottaviani L, Idrissi H, Lancin M, Martinuzzi S, Pichaud B (2004) Structural characterisation of 4H-SiC substrates by cathodoluminescence and X-ray topography. *Eur Phys J Appl Phys* 27(1–3):231–233
78. Weyher JL, Lazar S, Borysiuk J, Pernot J (2005) Defect-selective etching of SiC. *Physica Status Solidi (a)* 202(4):578–583
79. Isshiki T, Hasegawa M, Sato T, Kobayashi K, Miyaki A, Iyoki M, Yamaoka T, Onuki K (2018) Observation of a latent scratch on chemo-mechanical polished 4H-SiC wafer by mirror projection electron microscopy. In: *Materials science forum*, vol 924. Trans Tech Publications Ltd, pp 543–546
80. Senzaki J, Hayashi S, Yonezawa Y, Okumura H (2018) Challenges to realize highly reliable SiC power devices: from the current status and issues of SiC wafers. In: 2018 IEEE international reliability physics symposium (IRPS). IEEE, pp 3B–3
81. Hassan J, Henry A, McNally PJ, Bergman JP (2010) Characterization of the carrot defect in 4H-SiC epitaxial layers. *J Cryst Growth* 312(11):1828–1837
82. Ohira K, Isshiki T, Sako H, Hasegawa M, Kobayashi K, Onuki K (2020) Review and detail classification of stacking faults in 4H-SiC epitaxial layer by mirror projection Electron microscopy. In: *Materials science forum*, vol 1004. Trans Tech Publications Ltd, pp 314–320
83. Hassan J, Henry A, Ivanov IG, Bergman JP (2009) In-grown stacking faults in 4 H-SiC epilayers grown on off-cut substrates. *J Appl Phys* 105(12):123513
84. Guo J, Yang Y, Raghothamachar B, Kim T, Dudley M, Kim J (2017) Understanding the microstructures of triangular defects in 4H-SiC homoepitaxial. *J Cryst Growth* 480:119–125

85. Li J, Meng C, Yu L, Li Y, Yan F, Han P, Ji X (2020) Effect of various defects on 4H-SiC Schottky diode performance and its relation to epitaxial growth conditions. *Micromachines* 11(6):609
86. Kim HK, Kim SI, Kim S, Lee NS, Shin HK, Lee CW (2020) Relation between work function and structural properties of triangular defects in 4H-SiC epitaxial layer: Kelvin probe force microscopic and spectroscopic analyses. *Nanoscale* 12(15):8216–8229
87. Chen B, Matsuhata H, Sekiguchi T, Ichinoseki K, Okumura H (2012) Surface defects and accompanying imperfections in 4H-SiC: optical, structural and electrical characterization. *Acta Mater* 60(1):51–58
88. Das H, Sunkari S, Justice J, Pham H, Park G, Seo YH (2020) Statistical analysis of killer and non-killer defects in SiC and the impacts to device performance. In: *Materials science forum*, vol 1004. Trans Tech Publications Ltd, pp 458–463
89. Katsuno T, Watanabe Y, Fujiwara H, Konishi M, Yamamoto T, Endo T (2011) Effects of surface and crystalline defects on reverse characteristics of 4H-SiC junction barrier Schottky diodes. *Jpn J Appl Phys* 50:04DP04
90. Sozzi G, Puzanghera M, Menozzi R, Nipoti R (2019) The role of defects on forward current in 4H-SiC p-n diodes. *IEEE Trans Electron Devices* 66(7):3028–3033
91. Li L, Yan H, Li J, Li Q, Zhu T, Wu H, Liu R, Jin R, Wu J (2021) Effect of wafer defects on electrical properties and yields of SiC Devices. *J Phys Conf Ser* 2033(1):012095
92. Senzaki J, Kojima K, Kato T, Shimozato A, Fukuda K (2006) Correlation between reliability of thermal oxides and dislocations in -type 4H-SiC epitaxial wafers. *Appl Phys Lett* 89:022909
93. Singh R (2006) Reliability and performance limitations in SiC power devices. *Microelectron Reliab* 46(5–6):713–730
94. Neudeck PG, Powell JA (1994) Performance limiting micropipe defects in silicon carbide wafers. *IEEE Electron Device Lett* 15(2):63–65
95. Van Brunt E, Burk A, Lichtenwalner DJ, Leonard R, Sabri S, Gajewski DA, Mackenzie A, Hull B, Allen S, Palmour JW (2018) Performance and reliability impacts of extended epitaxial defects on 4H-SiC power devices. In: *Materials science forum*, vol 924. Trans Tech Publications Ltd, pp 137–142
96. Chung JE, Chen J, Ko PK, Hu C, Levi M (1991) The effects of low-angle off-axis substrate orientation on MOSFET performance and reliability. *IEEE Trans Electron Devices* 38(3):627–633
97. Lebedev AA (1999) Deep level centers in silicon carbide: a review. *Semiconductors* 33:107–130
98. Fujiwara H, Naruoka H, Konishi M, Hamada K, Katsuno T, Ishikawa T, Watanabe Y, Endo T (2012) Relationship between threading dislocation and leakage current in 4H-SiC diodes. *Appl Phys Lett* 100:242102
99. Katsuno T, Watanabe Y, Fujiwara H, Konishi M, Naruoka H, Morimoto J, Morino T, Endo T (2011) Analysis of surface morphology at leakage current sources of 4H-SiC Schottky barrier diodes. *Appl Phys Lett* 98:222111
100. Saitoh H, Kimoto T, Matsunami H (2004) Origin of leakage current in SiC Schottky barrier diodes at high temperature. *MSF* 457–460:997–1000
101. Grekov A, Zhang Q, Fatima H, Agarwal A, Sudarshana T (2008) Effect of crystallographic defects on the reverse performance of 4H-SiC JBS diodes. *Microelectron Reliab* 48(10):1664–1668
102. Fujiwara H, Kimoto T, Tojo T, Matsunami H (2005) Characterization of in-grown stacking faults in 4H-SiC (0001) epitaxial layers and its impacts on high-voltage Schottky barrier diodes. *Appl Phys Lett* 87:051912
103. Lee K-Y, Huang Y-H (2012) An investigation on barrier inhomogeneities of 4H-SiC Schottky barrier diodes induced by surface morphology and traps. *IEEE Trans Electron Devices* 59(3):694–699
104. Wahab Q, Ellison A, Henry A, Janzén E, Hallin C, Di Persio J, Martinez R (2000) Influence of epitaxial growth and substrate-induced defects on the breakdown of 4H-SiC Schottky diodes. *Appl Phys Lett* 76(19):2725–2727
105. Lendenmann H, Dahlquist F, Bergman P, Bleichner H, Hallin C (2002) High-power SiC diodes: Characteristics, reliability and relation to material defects. In: *Materials science forum*, vol 389. Trans Tech Publications Ltd, pp 1259–1264
106. Kimoto T, Miyamoto N, Matsunami H (1999) Performance limiting surface defects in SiC epitaxial pn junction diodes. *IEEE Trans Electron Devices* 46(3):471–477
107. Stahlbush RE, Fatemi M, Fedison JB, Arthur SD, Rowland LB, Wang S (2002) Stacking-fault formation and propagation in 4H-SiC PiN diodes. *J Electron Mater* 31(5):370–375
108. Deretzis I, Camarda M, La Via F, La Magna A (2012) Electron backscattering from stacking faults in SiC by means of ab initio quantum transport calculations. *Phys Rev B* 85(23):235310
109. Ha S, Skowronski M, Lendenmann H (2004) Nucleation sites of recombination-enhanced stacking fault formation in silicon carbide p-i-n diodes. *J Appl Phys* 96:393–398
110. Fukuda K, Kinoshita A, Ohyanagi T, Kosugi R, Sakata T, Sakuma Y, Sakuma Y, Senzaki J, Minami A, Shimozato A, Suzuki T, Arai K (2010) Influence of processing and of material defects on the electrical characteristics of SiC-SBDs and SiC-MOSFETs. In: *Materials science forum*, vol 645. Trans Tech Publications Ltd, pp 655–660
111. Han L, Liang L, Kang Y, Qiu Y (2020) A review of SiC IGBT: models, fabrications, characteristics, and applications. *IEEE Trans Power Electron* 36(2):2080–2093
112. Kimoto T, Cooper JA (2014) *Fundamentals of silicon carbide technology: growth, characterization, devices and applications*. Wiley
113. Li J-L, Li Y, Wang L, Xu Y, Yan F, Han P, Ji X-L (2019) Influence of deep defects on electrical properties of Ni/4H-SiC Schottky diode. *Chin Phys B* 28:027303
114. Son NT, Zolnai Z, Janzén E (2003) Silicon vacancy related TV2center in 4H-SiC. *Phys Rev B* 68:205211
115. Orlinski SB, Schmidt J, Mokhov EN, Baranov PG (2003) Silicon and carbon vacancies in neutron-irradiated SiC: a high-field electron paramagnetic resonance study. *Phys Rev B* 67:125207
116. Lukin DM, Guidry MA, Vučković J (2020) Integrated quantum photonics with silicon carbide: challenges and prospects. *PRX Quantum* 1(2):020102
117. Ren N, Liu L, Wu J, Sheng K (2021) Plasma spreading layers: an effective method for improving surge and avalanche robustness of SiC devices. *IEEE Trans Electron Devices* 68(11):5687–5694
118. Choi PH, Kim YP, Kim MS, Ryu J, Baek SH, Hong SM, Jang JH (2021) Side-illuminated photoconductive semiconductor switch based on high purity semi-insulating 4H-SiC. *IEEE Trans Electron Devices* 68(12):6216–6221
119. Wang J, Liu Y, Yu S, Wang C, Ding L, Jiang N (2021) A novel double-sided cooling packaging structure of SiC-based half bridge module integrating the laminated busbar. *Microelectron Reliab* 126:114242
120. Arvanitopoulos A, Antoniou M, Li F, Jennings MR, Perkins S, Gyftakis KN, Lophitis N (2021) 3C-SiC-on-Si MOSFETs: overcoming material technology limitations. *IEEE Trans Ind Appl* 58(1):565–575
121. Pu S, Yang F, Vankayalapati B, Akin B (2021) Aging mechanisms and accelerated lifetime tests for SiC MOSFETs: an overview. *IEEE J Emerg Sel Top Power Electron* 10(1):1232–1254
122. Sampayan K, Sampayan S (2019) Wide bandgap photoconductive switches driven by laser diodes as a high-voltage mosfet replacement for bioelectronics and accelerator applications. In: *2019 IEEE pulsed power and plasma science (PPPS)*. IEEE, pp 1–4
123. Brunt EV, Cheng L, O'Loughlin M, Capell C, Jonas C, Lam K, Scozzie C (2014) 22 kV, 1 cm², 4H-SiC n-IGBTs with improved conductivity modulation. In: *2014 IEEE 26th international symposium on power semiconductor devices & IC's (ISPSD)*. IEEE, pp 358–361
124. Kawata A, Murayama K, Sumitani S, Harada S (2021) Design of automatic detection algorithm for dislocation contrasts in birefringence images of SiC wafers. *Jpn J Appl Phys* 60(SB):SBBD06
125. Leonard R, Conrad M, Van Brunt E, Giles J, Hutchins E, Balkas E (2020) From wafers to bits and back again: using deep learning to accelerate the development and characterization of SiC. In: *Materials science forum*, vol 1004. Trans Tech Publications Ltd, pp 321–327
126. Monno S, Kamada Y, Miwa H, Ashida K, Kaneko T (2018) Detection of defects on SiC substrate by SEM and classification using deep learning. In: *International conference on intelligent networking and collaborative systems*. Springer, Cham, pp 47–58
127. Friedrichs P (2007) Silicon carbide power devices-status and upcoming challenges. In: *2007 European conference on power electronics and applications*. IEEE, pp 1–11
128. Mitani T, Eto K, Komatsu N, Hayashi Y, Suo H, Kato T (2021) Reduction of threading screw dislocations in 4H-SiC crystals by a hybrid method

- with solution growth and physical vapor transport growth. *J Cryst Growth* 568:126189
129. Xie X, Peng Q, Chen G, Li J, Long J, Pan G (2021) Femtosecond laser modification of silicon carbide substrates and its influence on CMP process. *Ceram Int* 47(10)Part A:13322–13330
 130. Feng S, Zhang R, Huang C, Wang J, Jia Z, Wang J (2020) An investigation of recast behavior in laser ablation of 4H-silicon carbide wafer. *Mater Sci Semicond Process* 105:104701
 131. Lu C, Gao MM, Hu TT, Chen ZZ (2021) Modeling of excimer laser ablation of silicon carbide. *Phys Rev B* 104(11):115304
 132. Hattori J, Ito Y, Nagato K, Sugita N (2021) Investigation of damage generation process by stress waves during femtosecond laser drilling of SiC. *Precis Eng* 72:789–797
 133. Shen Y, Huang Y, Li Y, Zhao Q, Chen C, Liang Yao M (2021) Research on femtosecond infrared laser cutting 4H-SiC wafer. In: Sixteenth national conference on laser technology and optoelectronics, vol 11907. International Society for Optics and Photonics, p 119070X
 134. Zhou Z, He W, Zhang Z, Sun J, Schöner A, Zheng Z (2021) Characteristics of Ni-based ohmic contacts on n-type 4H-SiC using different annealing methods. *Nanotechnol Precis Eng* 4(1):013006
 135. Paneerselvam E, Choutapalli SH, Kumar HP, Vasa NJ, Nakamura D, Rao MR, Thomas T (2021) Simultaneous laser doping and annealing to form lateral p–n junction diode structure on silicon carbide films. *J Micro-manuf.* <https://doi.org/10.1177/25165984211016281>
 136. Bencherif H, Dehimi L, Eddine Athamena N, Pezzimenti F, Megherbi ML, Della Corte FG (2021) Simulation study of carbon vacancy trapping effect on low power 4H-SiC MOSFET performance. *Silicon* 13:1–9
 137. Dong P, Qin Y, Yu X, Xu X, Chen Z, Li L, Cui Y (2019) Electron radiation effects on the 4H-SiC PIN diodes characteristics: an insight from point defects to electrical degradation. *IEEE Access* 7:170385–170391
 138. Gadalla MN, Greenspon AS, Defo RK, Zhang X, Hu EL (2021) Enhanced cavity coupling to silicon vacancies in 4H silicon carbide using laser irradiation and thermal annealing. *Proc Natl Acad Sci* 118(12):e2021768118
 139. Wang C, Fang Z, Yi A, Yang B, Wang Z, Zhou L, Ou X (2021) High-Q microresonators on 4H-silicon-carbide-on-insulator platform for nonlinear photonics. *Light Sci Appl* 10(1):1–11
 140. Shi X, Fan W, Lu Y, Yi A, Ou X, Rottwitz K, Ou H (2021) Thermal oxidation assisted chemical mechanical polishing for low-loss 4H-SiC integrated photonic devices. In: 47th micro and nano engineering conference 2021
 141. Wu X, Fan T, Eftekhari AA, Hosseinnia AH, Adibi A (2021) High-Q ultra-sensitive integrated photonic sensors based on slot-ring resonator on a 3C-SiC-on-insulator platform. *Opt Lett* 46(17):4316–4319
 142. Soltamov VA, Soltamova AA, Baranov PG (2012) Room temperature coherent spin alignment of silicon vacancies in 4H- and 6H-SiC. *Phys Rev Lett* 108:226402
 143. Wellmann PJ (2018) Review of SiC crystal growth technology. *Semicond Sci Technol* 33(10):103001
 144. Ren N, Gao F, Wang H, Xia K, Song S, Yang H (2021) Water-induced effect on femtosecond laser layered ring trepanning in silicon carbide ceramic sheets using low-to-high pulse repetition rate. *Opt Commun* 496:127040
 145. Zimmer K, Ehrhardt M, Lorenz P, Wang X, Wang P, Sun S (2022) Etching of SiC–SiC-composites by a laser-induced plasma in a reactive gas. *Ceram Int* 48(1):90–95
 146. Usami Y, Imokawa K, Nohdomi R, Sunahara A, Mizoguchi H (2021) Adaptation of TCAD simulation in excimer laser doping. *Jpn J Appl Phys* 60(8):086502
 147. Mizoguchi H (2021) Structural changes of 4H-SiC. In: Excimer laser doping

Publisher's Note

Springer Nature remains neutral with regard to jurisdictional claims in published maps and institutional affiliations.

Submit your manuscript to a SpringerOpen[®] journal and benefit from:

- Convenient online submission
- Rigorous peer review
- Open access: articles freely available online
- High visibility within the field
- Retaining the copyright to your article

Submit your next manuscript at ► [springeropen.com](https://www.springeropen.com)
